Supporting Information for

A facile dopamine-mediated metal-catecholamine coating for therapeutic nitric oxide gas interface-catalytic engineering of vascular devices

Qiang Song,[a] Long Li,[b] Kaiqin Xiong,[a] Wenjie Tian,[c] Jing Lu,[d] Jin Wang,[a] Nan Huang,*[,a] Qiufen Tu,*[,a] and Zhilu Yang [a]

[a]Key Lab. of Advanced Technology for Materials of Education Ministry, School of Materials Science and Engineering, Southwest Jiaotong University, Chengdu, 610031, China.

[b]Institute of Environmental Engineering Technology, China Institute for Radiation Protection, Taiyuan, 030006, China.

[c]Cardiology Department, Sichuan Provincial People's Hospital & Sichuan Academy of Medical Sciences, Chengdu, Sichuan 610072, China.

[d]Anesthesiology Department,Sichuan Provincial People's Hospital & Sichuan Academy of Medical Sciences,Chengdu, Sichuan 610072, China.

E-mail addresses: huangnan1956@163.com; tuqiufen@swjtu.edu.cn

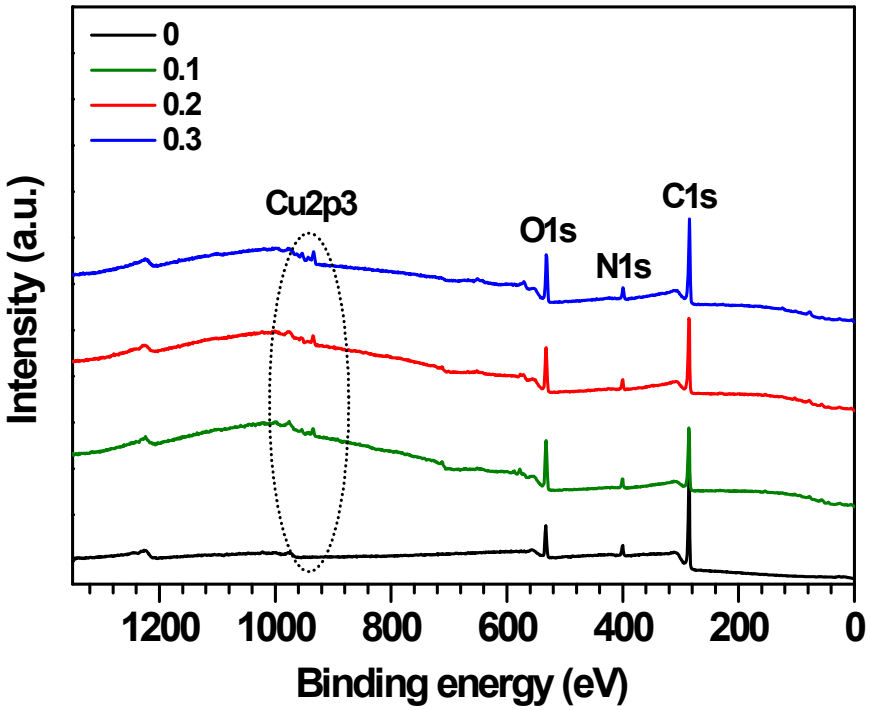

Fig. S1 XPS spectra of the Cu^{II}-DA coatings, which were prepared with different feeding concentrations of $CuCl_2 \cdot 2H_2O$ (0, 0.1, 0.2, and 0.3 mg/mL).

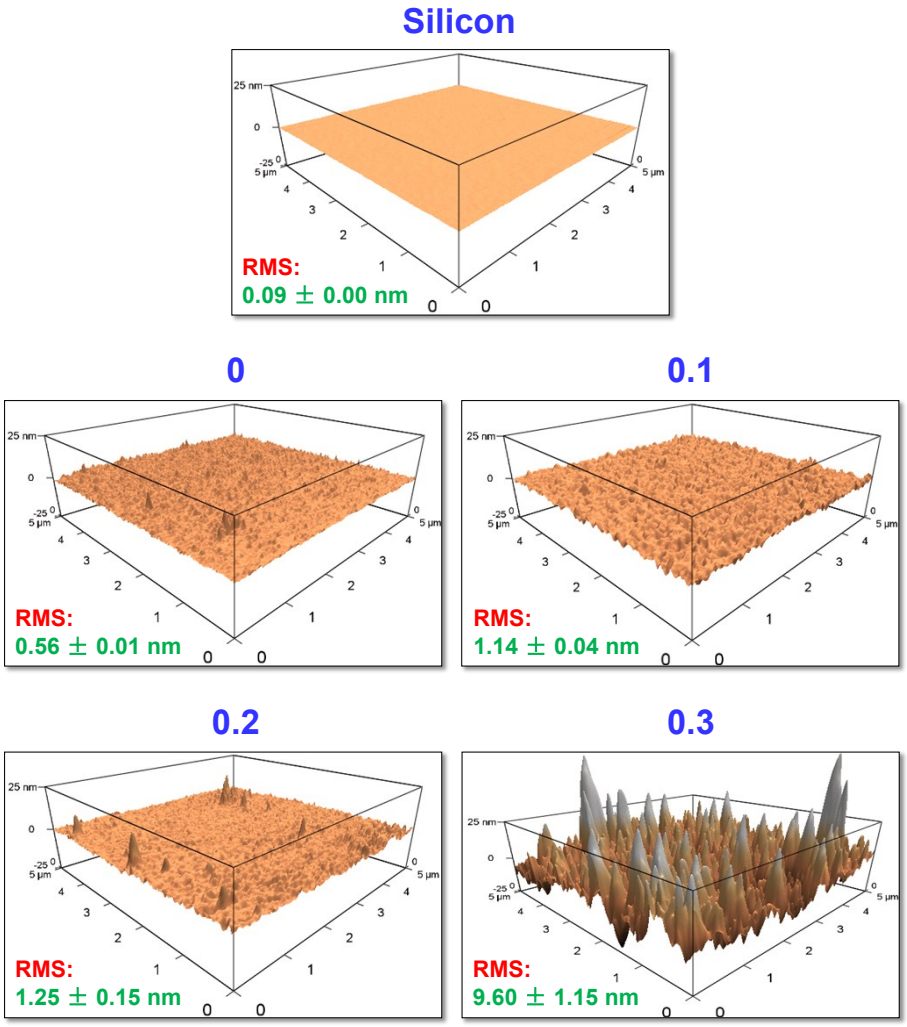

Fig. S2 Representative AFM images of silicon substrates modified with Cu^{II}-DA coatings, which were prepared with different feeding concentrations of $CuCl_2 \cdot 2H_2O$ (0, 0.1, 0.2, and 0.3 mg/mL).

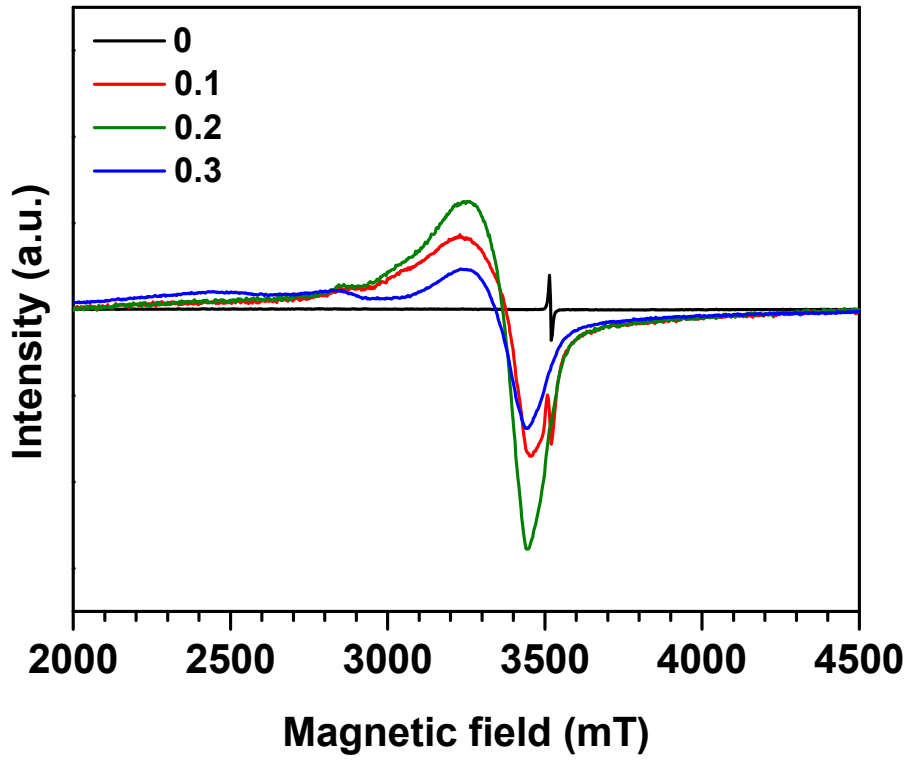

Fig. S3 EPR spectra of the Cu^{II}-DA coatings, which were prepared with different feeding concentrations of $CuCl_2 \cdot 2H_2O$ (0, 0.1, 0.2, and 0.3 mg/mL).

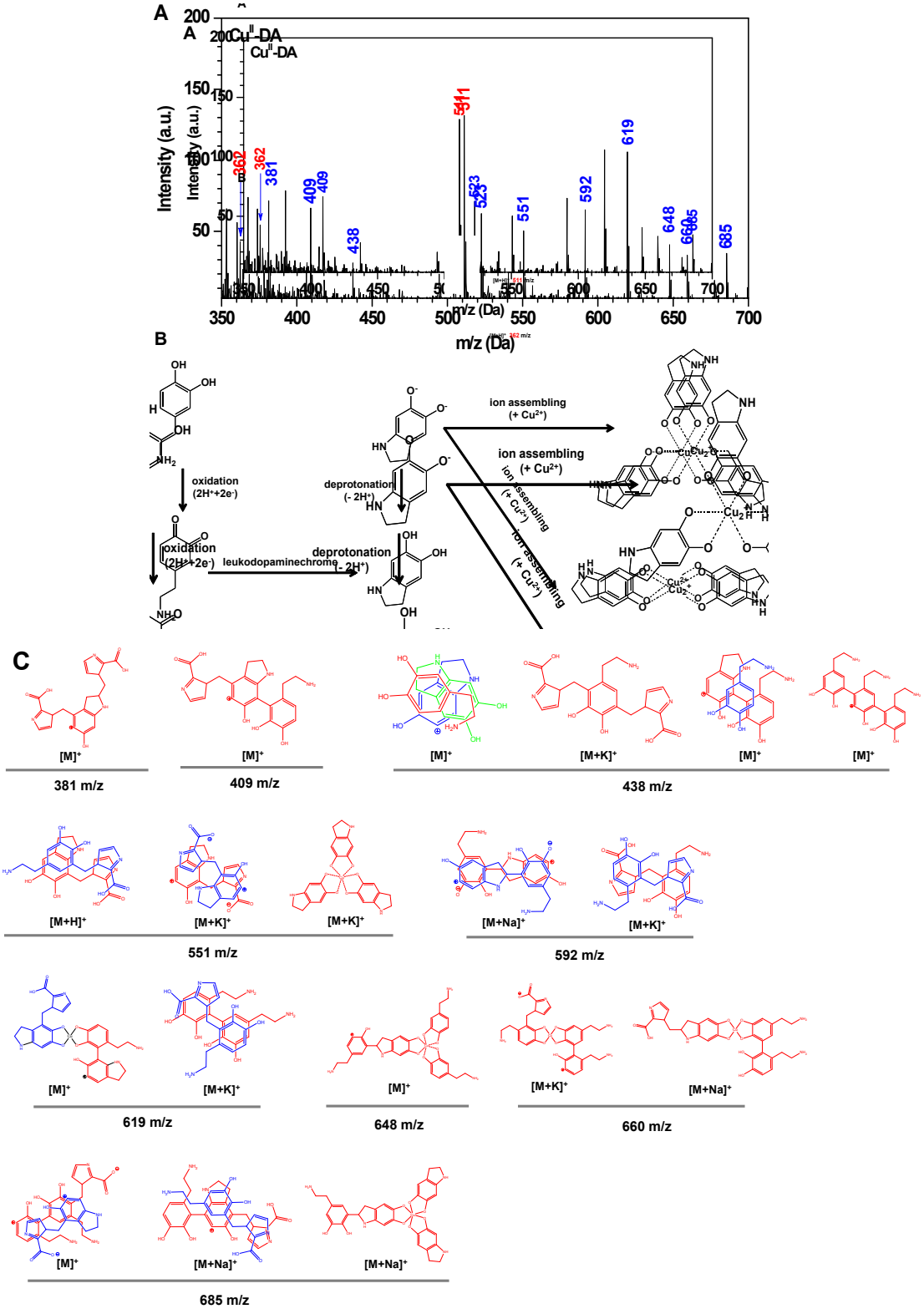

Fig. S4 (A) MALDI MS analysis of the Cu^{II}-DAcoating. (B) Possible chemical reactions between Cu^{II} and DA with a tetradentate and hexadentate chelating model. (C) Possible chemical structure assigned to some other obvious peaks.

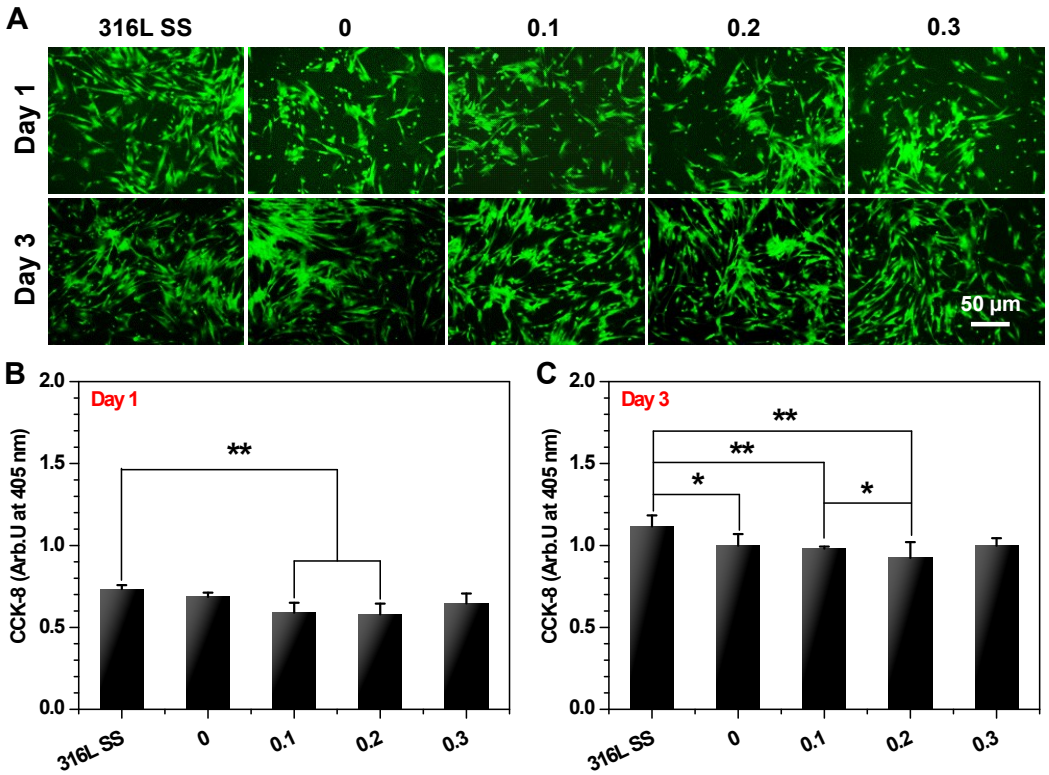

Fig. S5 Growth of HUASMCs cultured on different samples. (A) Fluorescence staining of HUASMCs incubated in cell culture media without NO donor for 1 and 3 days, respectively. (B) and (C) Growth analysis of HUASMCs using CCK-8. Data are presented as mean ± SD and analyzed by one-way ANOVA ($n = 4$, $^{*}p < 0.05$, and $^{**}p < 0.01$).

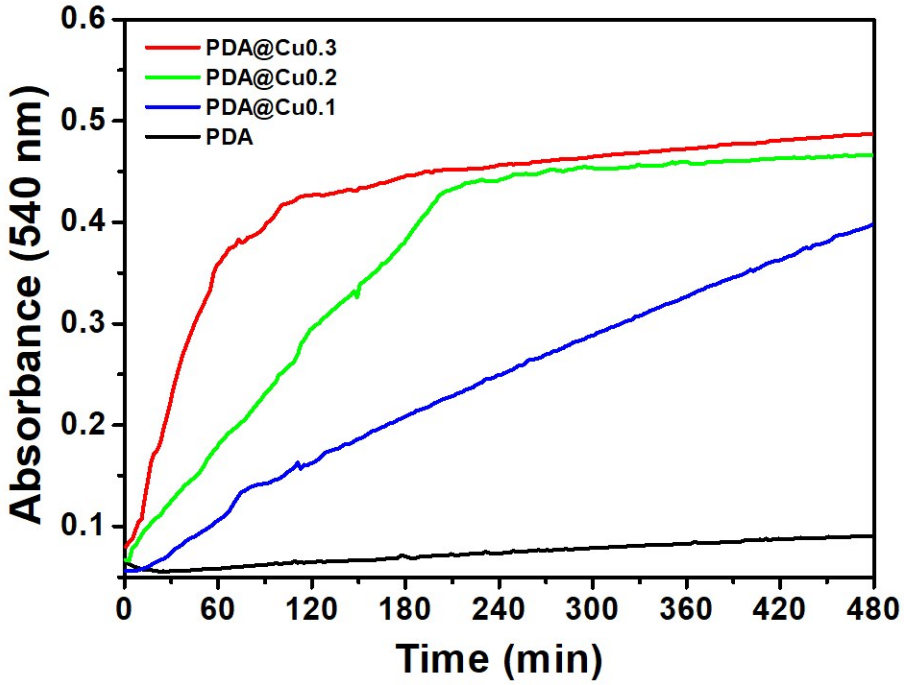

Fig. S6 Real-time catalytic release curve of the Cu^{II}-DA coatings (deposited on 24 well cell culture plates) with different feeding concentrations of $CuCl_2 \cdot 2H_2O$ (0, 0.1, 0.2, and 0.3 mg/mL). Each well was supplemented with 1 mL NO donor solution (10 μM GSNO and 10 μM GSH), the release of NO was reflected via OD value detected by enzyme labeling instrument by using Griess reagent.

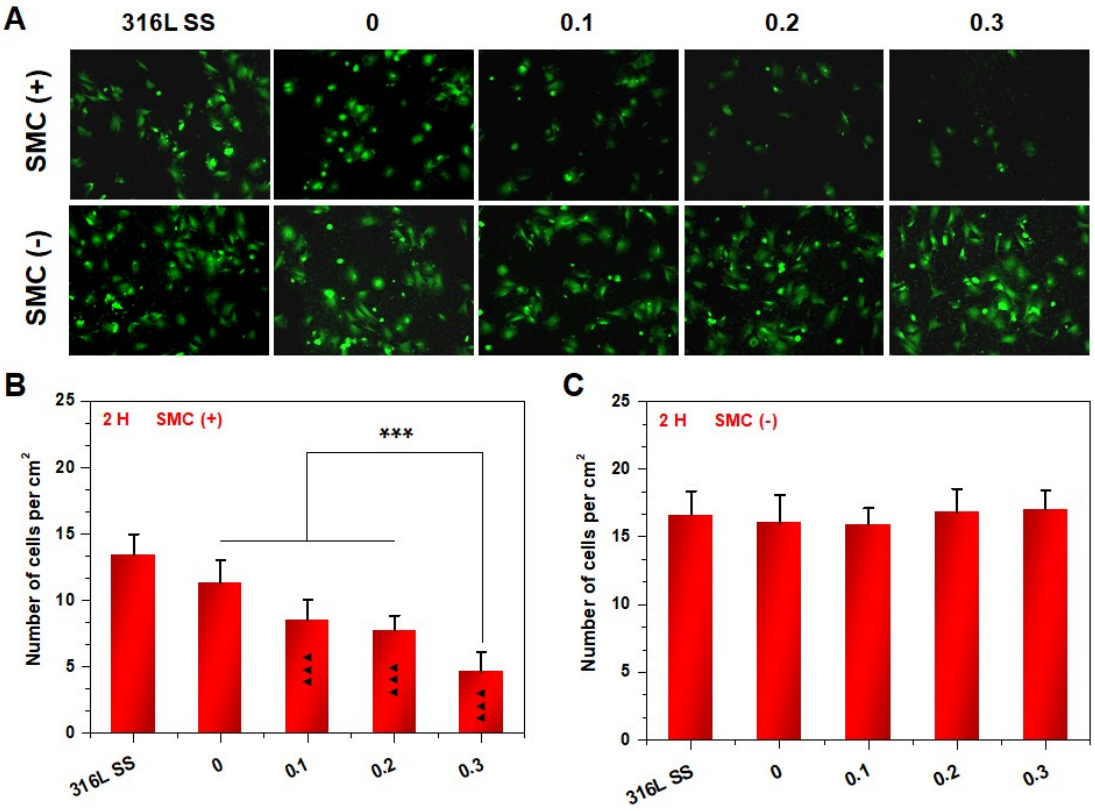

Fig. S7 Adhesion of HUASMCs on different samples after 2 h of culture in the presence and absence of NO donor. (A) Fluorescent images and (B, C) cell count and statistical analysis. Data are presented as mean ± SD and analyzed by one-way ANOVA (n = 4, ***p < 0.001, ▼▼▼p < 0.001 compared with 316L SS samples).

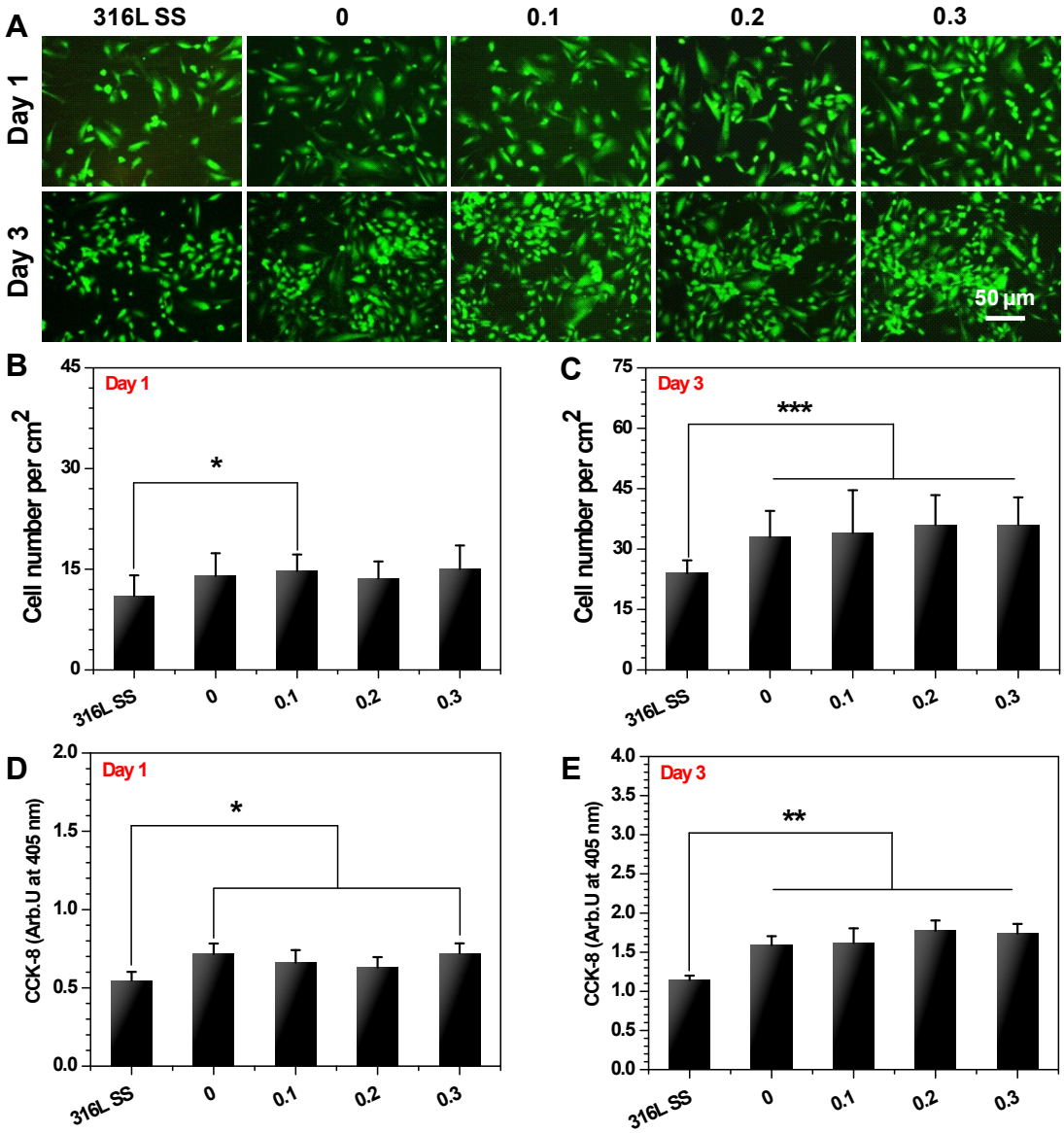

Fig. S8 Growth of HUVECs cultured on different samples. Fluorescence staining of HUVECs incubated in cell culture media without NO donor for 1 and 3 days, respectively (A). Number of HUVECs per cm^2 from fluorescence images (B, C). Growth analysis of HUVECs using CCK-8 (D, E). Data are presented as mean ± SD and analyzed by one-way ANOVA (n = 4, *$p < 0.05$, and **$p < 0.01$).

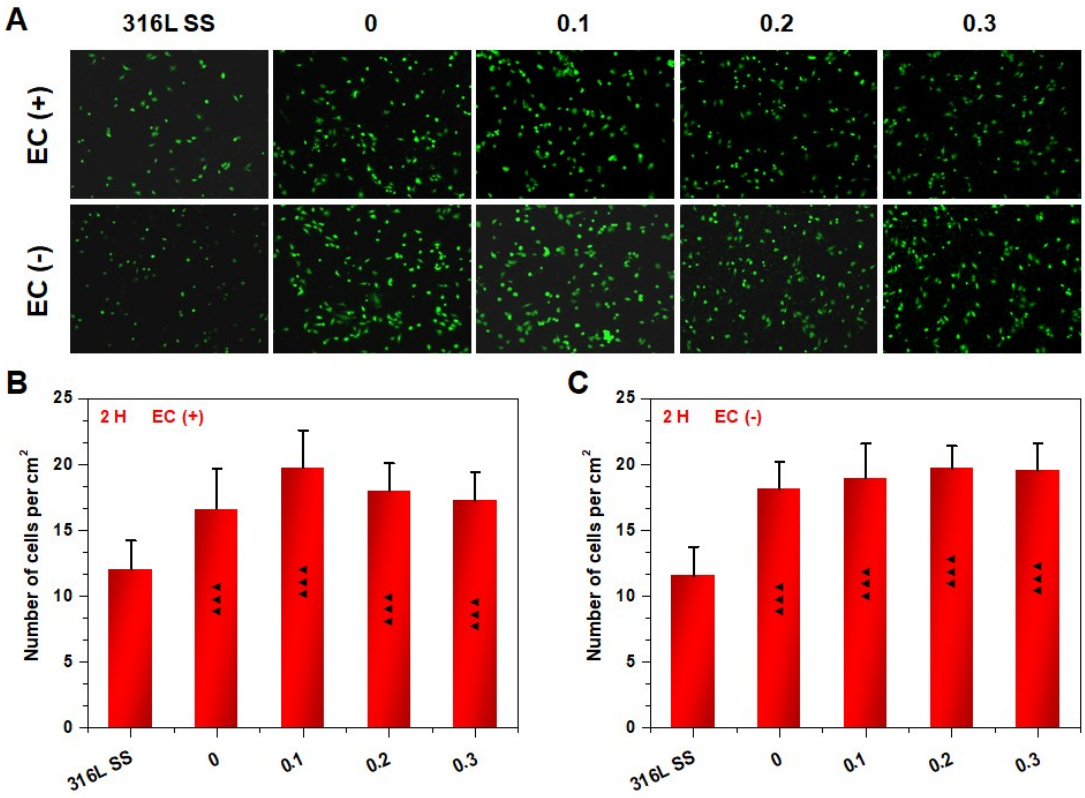

Fig. S9 Adhesion of HUVECs on different samples after 2 h of culture in the presence and absence of NO donor. (A) Fluorescent images and (B, C) cell count and statistical analysis. Data are presented as mean ± SD and analyzed by one-way ANOVA (n = 4, ▼▼▼$p < 0.001$ compared with 316L SS samples).

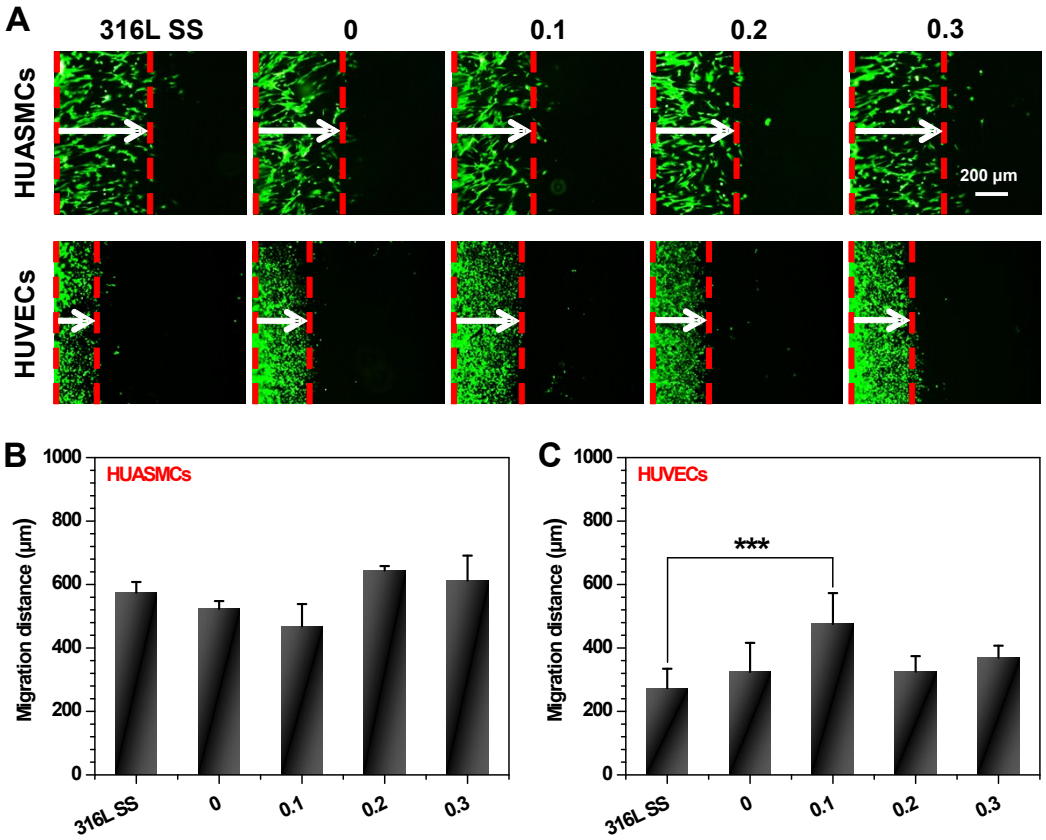

Fig. S10 Vascular cell migration. (A) Rhodamine staining of HUASMCs (top) and HUVECs (bottom) on different surfaces after culture in media without NO donor for 1 day. (A). Migration distance of HUASMCs (B) and HUVECs (C). Data are presented as mean ± SD (n=12) and analyzed by one-way ANOVA (***$p < 0.001$).

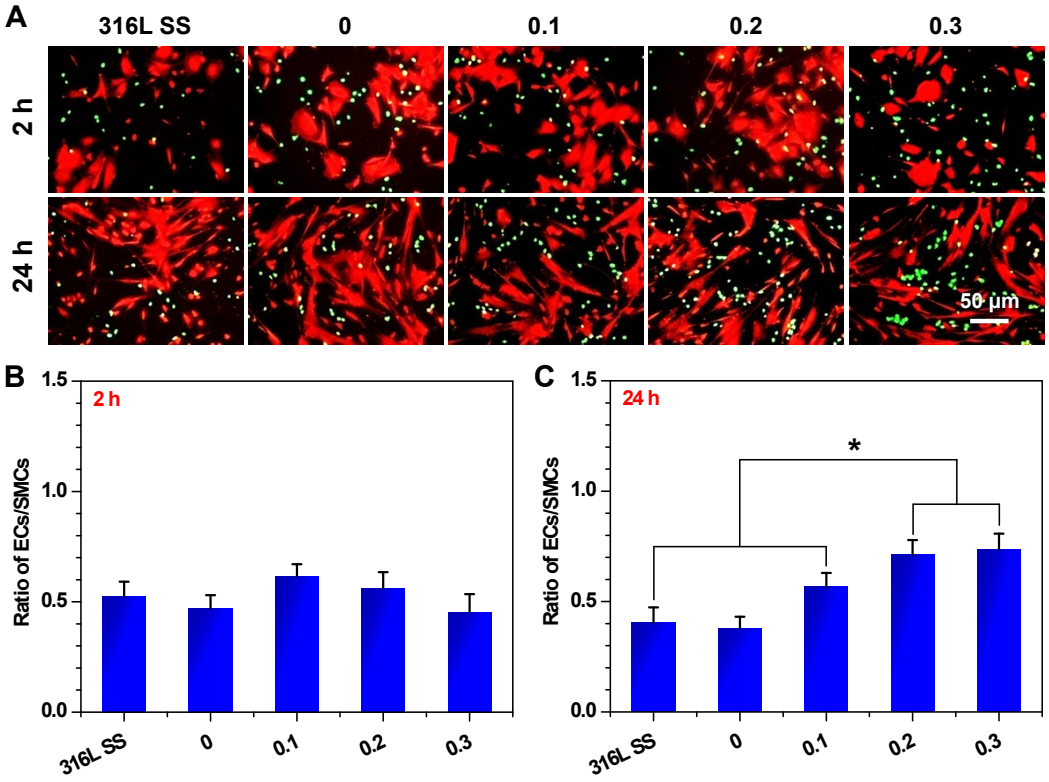

Fig. S11 Competitive adhesion and growth between HUASMCs and HUVECs on different samples after 2 and 24 h of culture in media without NO donor. (A) Fluorescence staining of HUASMCs using CMTMR (red) and HUVECs using CMFDA (green) grown on different surfaces. The ratio of HUVECs/HUASMCs on different surfaces for 2 h (B) and 24 h (C). Data are presented as mean ± SD and analyzed by one-way ANOVA (n = 8, *p < 0.05).

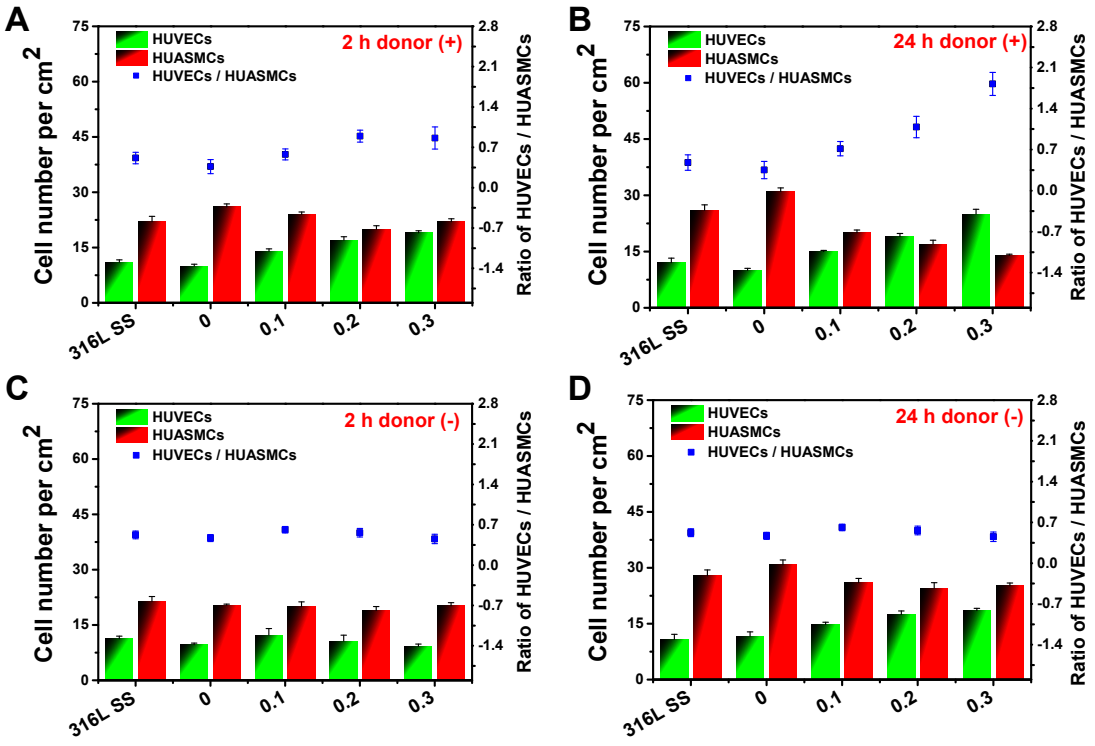

Fig. S12 Competitive adhesion between HUVECs and HUASMCs on different samples after 2 and 24 h of culture in both the presence and absence of NO donor. The figure shows the number of HUVECs and HUASMCs, and the ratio of the two cells, respectively.

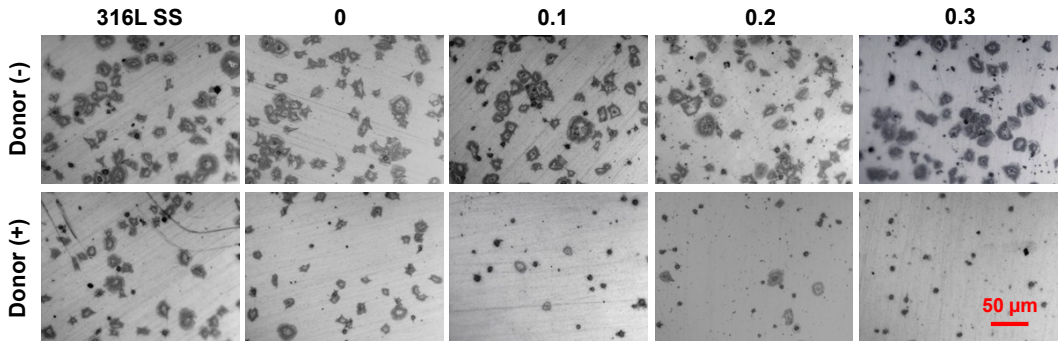

Fig. S13 Optical microscope images of the platelets adhered on different surfaces after culture in PRP without and with NO donor (10 μM GSNO, 10 μM GSH) for 15 min.

Table S1. Atomic compositions of the Cu^{II}-DA coatings fabricated using different feeding concentration of $CuCl_2 \cdot 2H_2O$.

Feeding concentration of $CuCl_2 \cdot 2H_2O$ (mg/mL)	Content [at.%]			
	C	N	O	Cu
0	81.7	5.9	12.4	0
0.1	73.6	6.8	18.6	1.1
0.2	73.7	6.1	18.8	1.4
0.3	73.3	7.2	17.8	1.7